DRIVING MECHANICAL ROBOTS THROUGH LINEAR ACTUATORS

Alexandra M.S.F. Galhano, J.A. Tenreiro Machado

Institute of Engineering of the Polytechnic Institute of Porto
Dept. of Electrical Engineering, Rua de S. Tomé, 4200 Porto, Portugal
Fax: +351-2-821159; e-mail: {afg, jtm}@dee.isep.ipp.pt

Abstract: Present day mechanical manipulators have poor performances when compared with the human arm. In fact, joint-driven manipulators are not efficient due to the high actuator requirements imposed by the transients of the operational tasks. Muscle-actuated arms are superior because the anatomic levers adapt the manipulating exigencies to the driving linear actuators. The kinematic analysis of these systems highlights its main properties and constitutes a step towards the design of new mechanical biological-like robotic structures adopting linear actuators replacing the standard rotational joint-driving motor systems.

1.- INTRODUCTION

The low performances of robotic manipulators, when compared with the human arm, motivated the development of new mechanical structures. Research in this area lead to the development of mathematical and computer models of the kinematic and dynamic phenomena [1–7]. Nevertheless, clear guidelines towards the implementation of optimal manipulating structures are still lacking. Joint-driven manipulators, with standard actuators, are not well adapted to the transients imposed by the robotic applications [8–9]. Alternative structures having muscle-like actuators and appropriate mechanical levers [10–15], may allow more efficient manipulating structures.

This paper investigates the arm biomechanics and evaluates its influence upon the driving actuators. In this perspective the article is organized as follows. Section two formulates a geometrical model of the human arm and section three analyzes the performances of muscle-actuated manipulators. Motivated by the results, section four studies the development and control of linear actuators. Finally, section five outlines the main conclusions.

2.- A GEOMETRIC MODEL OF THE HUMAN ARM

Extensive studies [16–25] have been carried out on the analysis of the human arm, still there are not definite conclusions. Therefore, in order to simplify matters, only the arm motion in the sagittal plane is considered (Figs. 1 to 3).

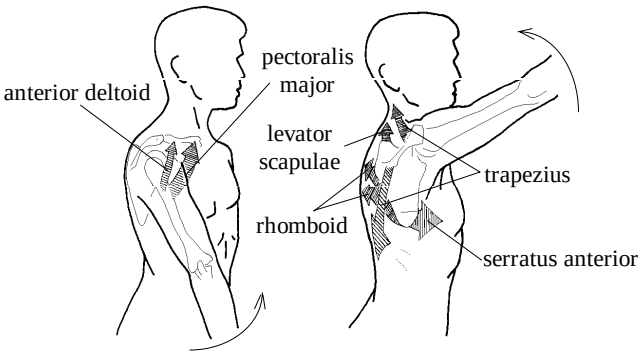

Fig. 1: Shoulder joint during the flexion in the sagittal plane.

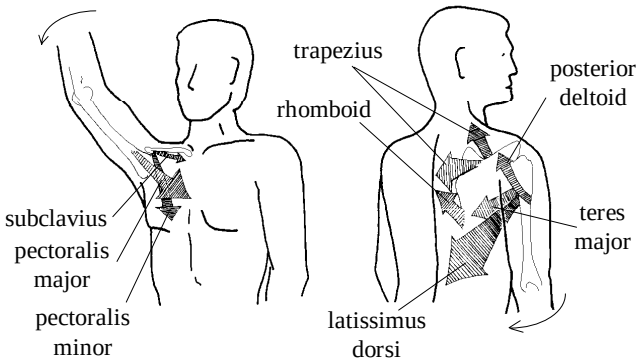

Fig. 2: Shoulder joint during the extension in the sagittal plane.

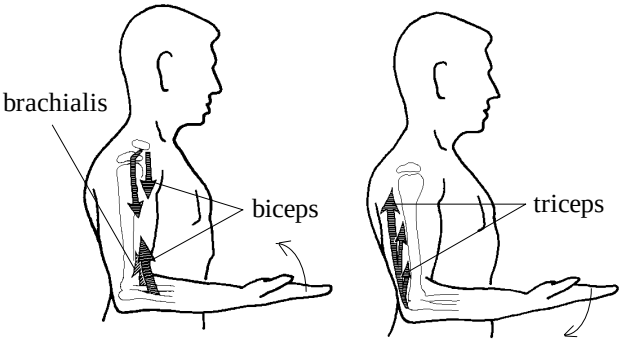

Fig. 3: Elbow joint during the flexion and extension in the sagittal plane.

A simple observation reveals that, at the biomechanical level, the human arm is driven by two main articulations: the shoulder and the elbow. Due to the fact that muscles are unidirectional actuators, articulations are driven by pairs of antagonist muscles activated alternatively during flexion and extension.

Figure 4 shows a simplified geometrical model of this mechanism in the sagittal plane [26–27]. The anterior and posterior deltoids drive the shoulder joint and have insertions both on the humerus and the pulley structure. Here, the pulley accounts for the scapulae, the clavicle, the sternum and the trunk, and has an independent motion (q_{01} for flexion and q_{02} for extension) of the arm movement (q_1). In this sense, the relative position of the arm and the pulley is controlled by the pair of deltoids, while the absolute position of the pulley is controlled by muscles such as the serratus anterior, the trapezius and the rhomboids.

The elbow reveals a simpler structure. For the movement of the elbow in the sagittal plane (q_2), the main muscles involved are the biceps brachii and the triceps brachii while, to a smaller significance, we can mention the brachialis and the anconeus.

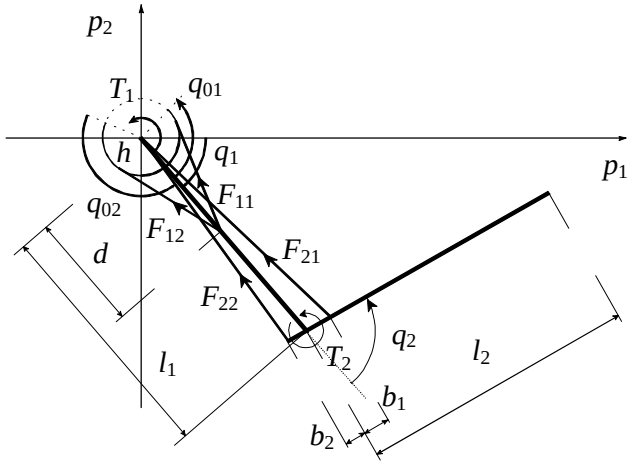

Fig. 4: Model of the human arm in the sagittal plane for the shoulder and the elbow structures.

In what concerns the relations between positions, velocities and accelerations on the operational and joint spaces (*i.e.* $\{\mathbf{q},\dot{\mathbf{q}},\ddot{\mathbf{q}}\}$ and $\{\mathbf{p},\dot{\mathbf{p}},\ddot{\mathbf{p}}\}$, respectively), for the structure we have the conventional robot inverse kinematics:

$$\begin{bmatrix} q_1 \\ q_2 \end{bmatrix} = \begin{bmatrix} tan^{-1}\left(\frac{p_2}{p_1}\right) - tan^{-1}\left(\frac{l_2 S_2}{l_1 + l_2 C_2}\right) \\ cos^{-1}\left(\frac{{p_1}^2 + {p_2}^2 - {l_1}^2 - {l_2}^2}{2 l_1 l_2}\right) \end{bmatrix} \tag{1a}$$

$$\begin{bmatrix} \dot{q}_1 \\ \dot{q}_2 \end{bmatrix} = \frac{1}{l_1 l_2 S_2} \begin{bmatrix} l_2 C_{12} & l_2 S_{12} \\ -l_1 C_1 - l_2 C_{12} & -l_1 S_1 - l_2 S_{12} \end{bmatrix} \begin{bmatrix} \dot{p}_1 \\ \dot{p}_2 \end{bmatrix} \tag{1b}$$

$$\begin{aligned} \begin{bmatrix} \ddot{q}_1 \\ \ddot{q}_2 \end{bmatrix} &= \frac{1}{l_1 l_2 S_2} \begin{bmatrix} l_2 C_{12} & l_2 S_{12} \\ -l_1 C_1 & -l_1 S_1 \end{bmatrix} \begin{bmatrix} \ddot{p}_1 \\ \ddot{p}_2 \end{bmatrix} + \\ &+ \frac{1}{l_1 l_2 S_2} \begin{bmatrix} l_1 l_2 C_2 & {l_2}^2 \\ -{l_1}^2 & -l_1 l_2 C_2 \end{bmatrix} \begin{bmatrix} {\dot{q}_1}^2 \\ {\dot{q}_{12}}^2 \end{bmatrix} \end{aligned} \tag{1c}$$

Nevertheless, for the muscle-driven structure depicted in Fig. 1 we have a further kinematic transformation between the joint space and the actuator space $\{\mathbf{z},\dot{\mathbf{z}},\ddot{\mathbf{z}}\}$.

For the shoulder articulation we can derive the expressions of the actuators range of motion, displacements (z_{1i}), velocities ($\dot{z}_{1i}$) and accelerations ($\ddot{z}_{1i}$) both for the anterior ($i = 1$) and the posterior ($i = 2$) deltoids. In this case, the relationship between q_1 and q_{01} or q_{02} obeys a kinematic control scheme according with the equations:

$$q_{01} = \begin{cases} 0.528\pi - 0.5 q_1 & -2\pi/3 \le q_1 < -\pi/2 \\ 0.278\pi - q_1 & -\pi/2 \le q_1 < -\pi/6 \\ 0.361\pi - 0.5 q_1 & -\pi/6 \le q_1 < \pi/6 \\ 0.411\pi - 0.8 q_1 & \pi/6 \le q_1 \le 4\pi/9 \end{cases} \tag{2a}$$

$$q_{02} = \begin{cases} 1.083\pi - 0.5 q_1 & -2\pi/3 \le q_1 < -\pi/2 \\ 0.833\pi - q_1 & -\pi/2 \le q_1 < -\pi/6 \\ 0.917\pi - 0.5 q_1 & -\pi/6 \le q_1 < \pi/6 \\ 0.75\pi + 0.5 q_1 & \pi/6 \le q_1 \le 4\pi/9 \end{cases} \tag{2b}$$

These expressions represent a compromise for the minimization of the requirements posed to the pulley and arm actuators, respectively. Moreover, for the flexion and extension there are different situations for the interaction of the pulley and the muscles. For the flexion we have two distinct cases (*h* and *d* are geometrical parameters):

- For $-2\pi/3 \le q_1 < -\pi/18$ the anterior deltoid is wound around the pulley, yielding:

$$z_{11} = h\left[q_{01} - \sin^{-1}\left(\sqrt{d^2 - h^2}\,/\,d\right)\right] + \sqrt{d^2 - h^2} \tag{3a}$$

$$\dot{z}_{11} = h\dot{q}_{01} \tag{3b}$$

$$\ddot{z}_{11} = h\ddot{q}_{01} \tag{3c}$$

• For $-\pi/18 \le q_1 \le 4\pi/9$ the anterior deltoid is acting freely (*i.e.* is not wound around the pulley) leading to:

$$z_{11} = \sqrt{d^2 + h^2 - 2dhC_{01}} \quad (4a)$$

$$\dot{z}_{11} = (dhS_{01}/z_{11})\dot{q}_{01} \quad (4b)$$

$$\ddot{z}_{11} = \frac{dh}{z_{11}}\left[\left(\frac{z_{11}{}^2 C_{01} - dhS_{01}{}^2}{z_{11}{}^2}\right)\dot{q}_{01}{}^2 + S_{01}\ddot{q}_{01}\right] \quad (4c)$$

For the extension we a have a single case where the posterior deltoid is wound around the pulley through the total range of motion $-2\pi/3 \le q_1 \le 4\pi/9$:

$$z_{12} = h\left[2\pi - q_{02} - sen^{-1}\left(\sqrt{d^2 - h^2}/d\right)\right] + \sqrt{d^2 - h^2} \quad (5a)$$

$$\dot{z}_{12} = -h\dot{q}_{02} \quad (5b)$$

$$\ddot{z}_{12} = -h\ddot{q}_{02} \quad (5c)$$

For the elbow articulation acting in the sagittal plane ($0 \le q_2 \le \pi$), we can also derive the expressions for the displacements, velocities and accelerations (z_{2i}, $\dot{z}_{2i}$, $\ddot{z}_{2i}$) for the biceps brachii and triceps brachii (i = 1, 2), yielding:

$$z_{2i} = \sqrt{l_1{}^2 + b_i{}^2 + 2l_1 b_i C_2} \quad (6a)$$

$$\dot{z}_{2i} = -(l_1 b_i S_2 / z_{2i})\dot{q}_2 \quad (6b)$$

$$\ddot{z}_{2i} = -\frac{l_1 b_i}{z_{2i}}\left\{C_2 + l_1 b_i\left(\frac{S_2}{z_{2i}}\right)^2 \dot{q}_2{}^2 + S_2\ddot{q}_2\right\} \quad (6c)$$

where b_i is a parameter.

Comparing the equations (1) to (6) we conclude that the elbow muscle velocities (6b) compensate the factor $S_2{}^{-1}$, present in the conventional inverse kinematics (1b) of joint-actuated systems, that degrades the robot performances near singular points.

3.- KINEMATIC PERFORMANCE OF MUSCLE-ACTUATED ARMS

In this section we analyze the kinematics performances of muscle-actuated arms. We must note that we are not modeling the muscle properties but, in fact, we are proceeding in the opposite way. By other words, we describe the task requirements and the manipulator structure and we study its effect on the actuators. In this perspective, we assume that natural evolution should lead to muscles having properties well matched to the requirements.

In the experiments we "stimulate" the system through simple trajectories in the operational space and we compare the actuator kinematic variables for the joint-driven and muscle-driven robotics structures. In order to test the biomechanical model we decided to move the arm according with two different linear trajectories in the operational space:

$s_1 : (p_{1a}, p_{2a}) \equiv (0.01, 0) \rightarrow (p_{1b}, p_{2b}) \equiv (0.01, 0.30)$
$s_2 : (p_{1a}, p_{2a}) \equiv (0.30, 0) \rightarrow (p_{1b}, p_{2b}) \equiv (0.30, 0.30)$

where (p_{1a}, p_{2a}) and (p_{1b}, p_{2b}) are the coordinates of the initial and final trajectory points, respectively.

Trajectory s_1 starts near the singular point (0,0) while s_2 is less demanding because is far away from singularities. Moreover, the trajectories have identical time evolution:

$$s_i : (p_{1a}, p_{2a}) \rightarrow (p_{1b}, p_{2b}) \quad (7a)$$

$$s(t) = \frac{D}{T}\left[t - \frac{T}{2\pi} sen\left(\frac{2\pi}{T}t\right)\right] \quad (7b)$$

$$D = \sqrt{(p_{1a} - p_{1b})^2 + (p_{2a} - p_{2b})^2} \quad (7c)$$

where T is the time duration of the movement.

Figure 5 compares the time evolution of $\{q_i(t), \dot{q}_i(t), \ddot{q}_i(t)\}$ and $\{z_{i1}(t), \dot{z}_{i1}(t), \ddot{z}_{i1}(t)\}$ for s_1 and s_2 and $T = 1\,sec$. As expected, the results reveal that:

- The joint velocities and accelerations, $\dot{q}_i(t), \ddot{q}_i(t), (i = 1,2)$, attain higher levels for s_1 than for s_2.
- The displacements of the shoulder and elbow muscles, $z_{11}(t)$ and $z_{21}(t)$, are very limited for both trajectories, being amplified by the anatomic levers in order to produce the displacement in the operational space.
- The velocity of the elbow muscle, $\dot{z}_{21}(t)$, is not sensitive to the singularity near s_1 and gives similar values for s_2.
- The velocity of the shoulder muscle, $\dot{z}_{11}(t)$, is sensitive to the change from s_1 to s_2.
- The accelerations of the shoulder and elbow muscles, $\ddot{z}_{11}(t)$ and $\ddot{z}_{21}(t)$, are sensitive to the type of trajectory.

In conclusion, joint actuators, which are developments of standard driving machines that are designed for steady-state applications, are not well adapted to robotic applications. Manipulators must have transmission levers that adapt the operational space tasks to the muscle actuator requirements.

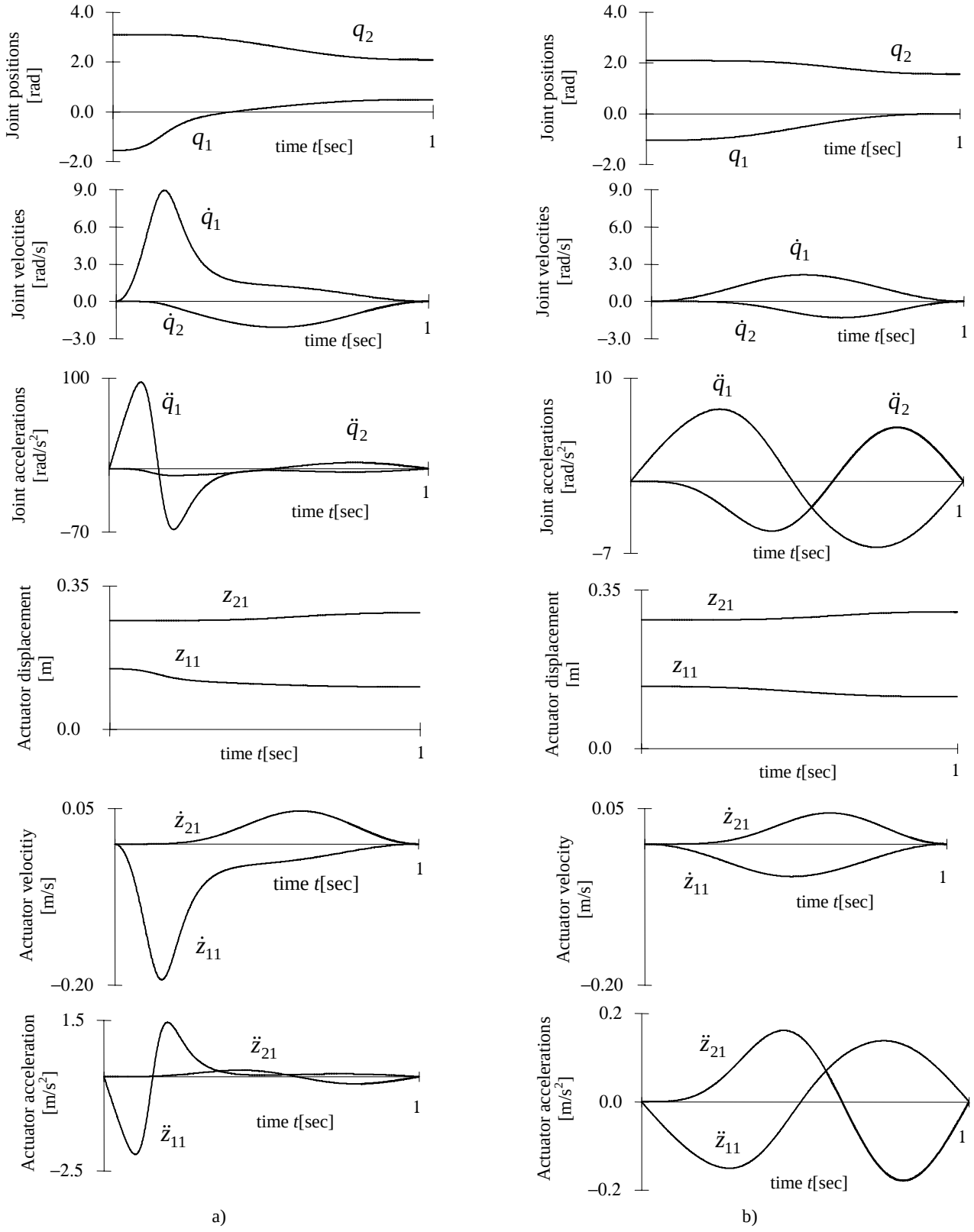

Fig. 5: Time evolution of positions, velocities and accelerations at the joints and muscles for trajectories:
a) $s_1 : (p_{1a},p_{2a}) \equiv (0.01, 0) \rightarrow (p_{1b},p_{2b}) \equiv (0.01, 0.30)$, b) $s_2 : (p_{1a},p_{2a}) \equiv (0.30, 0) \rightarrow (p_{1b},p_{2b}) \equiv (0.30, 0.30)$
$l_1 = 0.3$ *m*, $l_2 = 0.3$ *m*, $d = 0.126$ *m*, $h = 0.043$ *m*, $b_1 = 0.034$ *m*, $b_2 = -0.02$ *m*, $T = 1$ *sec.*

4.- LINEAR ACTUATORS FOR ROBOT MANIPULATORS

Muscle-driven manipulators require the development of appropriate linear actuators. Such actuators must provide high forces and high accelerations while driving small displacements. Moreover, in order to simplify the interface with the control system, an electrical actuator will be preferable. In this line of thought, a servo-solenoid is an electromagnetic equivalent of a muscle cell, and it can be modeled through the equations:

$$v = Ri + L\,\dot{i} + K_b\,\dot{x} \tag{7a}$$

$$f = K_f A\left(\frac{Ni}{x}\right)^2 \tag{7b}$$

Here R and L represent the resistance and inductance of the coil, N the number of turns, A and x are the area and length of the air gap in the magnetic circuit. The electrical voltage and current are v and i, the force exerted of the moving part of the solenoid is f and K_b and K_f are constants of proportionality.

As solenoids represent a mimic of muscles they can be associated in u series and in w parallels leading to the expressions for the total force F_{Total} and displacement x_{Total}:

$$F_{Total} = \sum_{i=1}^{w} \underset{j}{Min}\left(F_{ij}\right) \tag{8a}$$

$$x_{Total} = \sum_{j=1}^{u} \underset{i}{Min}\left(x_{ij}\right) \tag{8b}$$

Such associations allow the minimization of the actuator moving inertia and the allocation of different "cells" to distinct operating conditions (*e.g.* transient *versus* steady-state) in a hierarchical control system (Fig. 6).

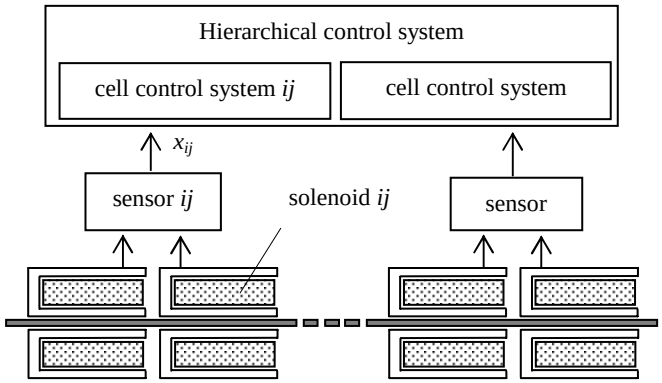

Fig. 6: Actuator hierarchical control system

In this perspective, the development of a linear electromagnetic actuator is currently under development (Fig. 7).

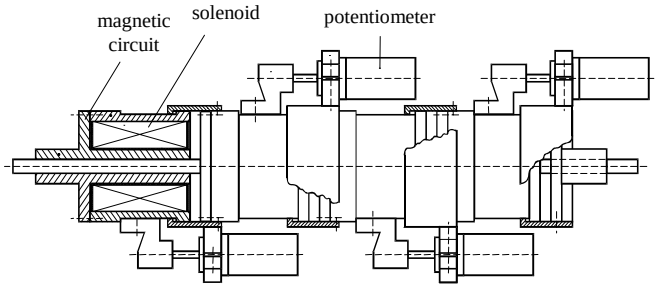

Fig. 7: Solenoid series for robotic application. Each "cell" has: R = 23.83 Ω, L = 1.88 *mH*, A = 19.35 10^{-4} m^2, Weight = 0.55 *Kg*.

In what concerns each "cell" control system it should be noted that equation (7b) poses stringent requirements due to the fact that:

- There is a negative dynamic characteristic that leads to an intrinsic unstable system;
- There is a high sensitivity of the actuator force f to variations of the air gap length x.

Figure 8 shows the block diagram of the solenoid control system for a load f_L with inertia J and friction B.

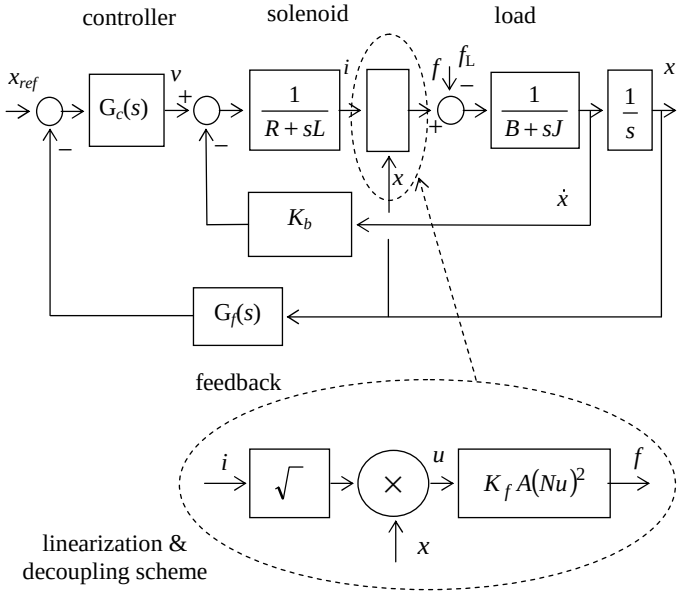

Fig. 8: Block diagram of the solenoid control system for a load f_L with inertia J and friction B.

Due to the complex dynamics revealed by equation (7b) the adoption of a decoupling and linearizing scheme leads to a closed-loop transfer function:

$$\frac{X(s)}{X_{ref}(s)} = \frac{K_i G_c(s)}{s[(R+sL)(B+Js)+K_i K_b]+K_i G_c(s) G_f(s)} \quad (9a)$$

$$\frac{X(s)}{F_L(s)} = \frac{R+sL}{s[(R+sL)(B+Js)+K_i K_b]+K_i G_c(s) G_f(s)} \quad (9b)$$

where $K_i = K_f A N^2$ and $G_c(s)$ and $G_f(s)$ are the transfer functions of the controller and feedback, respectively. Based on this model we can design the cell controller using standard linear system tools.

5. CONCLUSIONS

The paper presented the analysis of mechanical manipulators in the sagittal plane. Motivated by the kinesiological aspects of the human arm we demonstrate that biomechanical structures have better performances than standard robot manipulators. In fact, joint-actuated robotic structures are non-optimal because they have to support the direct impact of the operational requirements, while muscle-actuated arms are superior because they have anatomic levers and actuators more adapted to the transients required by the operational tasks. Therefore, these results are a step towards the design of a new generation of better manipulators structures and a new generation of linear muscle-like, low displacement high acceleration, actuators. In this perspective, it is proposed the adoption of solenoids as electromagnetic actuators that provide high forces and small displacements. Its dynamic characteristics are nonlinear and present challenging aspects in what concerns the control system that is presently under study.

References

[1] Tsai, Y. C., Soni, A. H.: Accessible region and synthesis of robot arms, ASME J. Mechanical Design, vol. 103, 1981, pp. 803–811.

[2] Asada, H.: A Geometrical representation of manipulator dynamics and its application to arm design, ASME J. Dynamic Syst., Meas., Contr., vol. 105, 1983, pp. 131–142.

[3] Asada, H., Youcef-Toumi, K.: Analysis and design of a direct-drive arm with a five-bar-link parallel mechanism, ASME J. Dynamic Syst., Meas., Contr., vol. 106, 1984, pp. 225–230.

[4] Yoshikawa, T.: Manipulability of robotic mechanisms, The Int. J. Robotics Research, vol. 4, 1985, pp. 3–9.

[5] Yoshikawa, T.: Analysis and design of articulated robot arms from the viewpoint of dynamic manipulability, Robotics Research, Proc. the Third Int. Symp., 1986, pp. 273–279.

[6] Yang, D.C.H., Tzeng, S.W.: Simplification and linearization of manipulator dynamics by the design of inertia distribution, The Int. J. Robotics Research, vol. 5, 1986, pp. 120–128.

[7] Youcef-Toumi, K., Asada, H.: The design of open-loop manipulator arms with decoupled and configuration-invariant inertia tensors, ASME J. Dynamic Syst., Meas., Contr., vol. 109, 1987, pp. 268–275.

[8] Galhano, A.F., Machado, J.T., Carvalho, J.M.: On the statistical modelling of mechanical manipulators, Proc. IFAC Symp. on Robot Control, 1991, pp. 15–20, Vienna, Austria.

[9] Machado, J. T., Galhano, A.F.; Statistical modelling of robotic manipulators, Journal Systems Analysis-Modelling-Simulation, vol. 12, 1993, pp. 101–123.

[10] An, K. N., Hui, F. C., Morrey, B. F., Linscheid, R. L., Chao, and E. Y.: Muscles across the elbow joint: a biomechanical analysis, J. of Biomechanics, vol. 14, 1981, pp. 659–669.

[11] Atkeson, C. G., Hollerbach, J. M.: Kinematic features of unrestrained vertical arm movements, J. Neuroscience, vol. 5, n. 9, 1985, pp. 2319–2330.

[12] Rossi, D, Domenici, C., Chiarelli P.: Analogs of biological tissues for mechanoelectrical transduction: tactile sensors and muscle-like actuators, Proc. NATO ARW on Sensors and Sensory Systems for Advanced Robots, 1986, Italy.

[13] Kuribayashi, K.: A new actuator of a joint mechanism using TiNi alloy wire, The Int. J. Robotics Research, vol. 4, 1986, pp. 47–58.

[14] Tatara, Y.: Mechanochemical actuators, Advanced Robotics, vol. 2, 1987, pp. 69–85.

[15] Caldwell, D. G., Taylor, P. M.: Artificial muscles as robotic actuators, Proc. IFAC Symp. on Robot Control, 1988, pp. 40.1–40.6, Karlsruhe, Germany.

[16] Kawato, M.: Adaptation and learning in control of voluntary movement by the central nervous system, Advanced Robotics, vol. 3, n. 3, 1989, pp. 229–249.

[17] Kinzel, G. L.: Reduction of instrumental linkage data for simple anatomical joint models, ASME J. Mechanical Design, vol. 104, 1982, pp. 218–226.

[18] Kendall, H.O., Kendall, F.P., Wadsworth, G.E., 1971, Muscles - Testing and function, The Williams & Wilkins Company, Baltimore, USA.

[19] Wells,K. F., Luttgens, K., 1976, Kinesiology - Scientific basis of human motion, W. B. Saunders Company,.

[20] Rasch, P. J., Burke, R. K., 1976, Kinesiology and applied anatomy - The science of human movement, Lea & Febiger, Philadelphia, USA.

[21] Fischer, L.P., Carret, J.P., Gonon, G.P., Dimnet, J.: Étude cinématique des mouvements de l'articulation scapulo-humérale (articulatio humeri), Rev. Chir. Orthop., vol. 63, 1977, pp. 108–112.

[22] Ito, N., Suzuki, R., Ishimura, K., Kuwahara, H.: Electromyographic study of shoulder joint, Proc. 4th Congress of I.S.E.K., 1979, pp. 22–23, Boston, USA.

[23] Kapandji, I., 1983, Physiologie articulaire - Schémas commentés de mécanique humaine - Tome 1, Membre supérieur, Maloine S. A., France.

[24] Hogan, N.: Adaptive Control of Mechanical impedance by coactivation of the antagonist muscles, IEEE Trans. Automat. Contr., vol. 29, n. 8, 1984, pp. 681–690.

[25] Akazawa, K., Fujii, K.: Theory of muscle contraction and motor control, Advanced Robotics, vol. 1, 1986, pp. 379–390.

[26] Galhano, A.F., Machado, J. T., Carvalho, J.M.: On the analysis of muscle-actuated manipulators, Proc. Fifth Int. Conf. on Advanced Robotics, 1991, pp. 67–71, Pisa, Italy.

[27] Galhano, A.F., Machado, J. T., Carvalho, J.M.: Statistical analysis of muscle-actuated manipulators, Proc. IEEE Int. Conf. on Robotics and Automation, 1992, pp. 332–337, Nice, France.